Climatic Effects on In-Situ Soil State Profiles Considering a Coupled Soil-Atmosphere Interaction Model

K.V. Bicalho, G.P.D. Vivacqua, Y.-J. Cui, C. Romanel

Abstract. The influence of soil-atmosphere interactions on an unsaturated soil in water-limited environment is investigated using a coupled heat-water flow model with a balance of net solar energy at earth's surface. The paper also presents the governing equations for soil-atmosphere interaction analysis which, although important, are still rare in geotechnical applications. Numerical results were obtained by approximating the governing partial differential equations through a 1D finite difference scheme representing the soil as a two-layer system. Soil state profiles (temperature, moisture and suction) were predicted using daily meteorological data collected in France, from 2004 to 2005. Parametric analyses estimated the effects on soil state profiles caused by changes in initial conditions (soil temperature), hydraulic properties (saturated hydraulic conductivity), model geometry (upper layer thickness), ratio of reflected to incident solar radiation (soil albedo) and characteristics of meteorological data (sampling frequency). For the investigated site, the zone of seasonal fluctuations (ZSF) where the moisture and corresponding suction profiles is influenced by climatic conditions is about 1.5 m. The results also show that calculated average month meteorological values as daily inputs modify significantly the ZSF (about 100%). Predicted soil temperature profiles were in good agreement with measured values.

Keywords: soil suction, soil temperature, soil moisture, unsaturated flow, evaporation, soil-atmosphere interaction.

1. Introduction

The exchange of water between the soil surface and the atmosphere is governed by two processes: infiltration and evaporation. The process of infiltration is reasonably well understood and depends primarily on the hydraulic conductivity of the soil while the evaporation flux from a soil surface is more difficult to quantify since it is a function of both the soil properties and climatic conditions.

To estimate evapotranspiration rates engineers have traditionally used the term potential evaporation, which may be understood as the maximum rate of evaporation from a pure water surface under given climatic conditions. The actual rate of evapotranspiration from a soil surface depends on the availability of water (Penman, 1948; Priestley & Taylor, 1972) and the maximum potential rate occurs only when the soil surface is fully saturated and water is present on the ground surface. The actual rate of evapotranspiration begins to decline once the soil surface becomes unsaturated and its determination is much more difficult because the analysis becomes indeterminate since there are more unknowns than unique equations.

The solution to this problem requires an approach where the flow of water from an evaporating unsaturated soil surface is represented as a coupled soil-atmosphere interaction (SAI) model taking into account the variation of suction along the soil profile due to spatial and temporal changes in soil moisture and temperature caused by microclimate conditions above the soil-atmosphere boundary. Studies with consideration of SAI effects in civil engineering problems are rare, especially in the geotechnical area, even though this subject has already been the topic of two Rankine Lectures (Blight, 1997; Gens, 2010).

Evapotranspiration from soil occurs in the form of combined liquid and vapour transport. Under field conditions it is not possible to separate evaporation from transpiration totally and the term actual evapotranspiration is used herein to describe the amount of total water loss. When the available soil moisture is depleted, the actual evapotranspiration will be limited by the monthly precipitation (lower limit) and the potential evapotranspiration (upper limit); in months when the potential evapotranspiration is less than the rainfall, the actual evapotranspiration is closer to the potential value (Fetter, 1994). Many regions have become drier and more drought-affected during recent decades (Dai *et al.*, 2004) and in water-limited regions (high soil suction) the ratio of the actual to the potential evaporation may be lower than 1 (Skidmore *et al.*, 1969; Blight, 1997).

Soil moisture varies depending on the actual evapotranspiration from soil surface which can be estimated by either field measurement based on water balance, energy balance or numerical analysis using meteorological data (Federer *et al.*, 1996). This former approach is desirable due to difficulties in direct measurements of soil suction us-

Kátia V. Bicalho, Ph.D., Associate Professor, Departamento de Engenharia Civil, Universidade Federal do Espírito Santo, Vitória, ES, Brazil. e-mail: kvbicalho@gmail.com.
Gabriel P.D. Vivacqua, M.Sc., Rechercher, Departamento de Engenharia Civil, Universidade Federal do Espírito Santo, Vitória, ES, Brazil. e-mail: gpd.vivacqua@hotmail.com.
Yu-Jun Cui, Ph.D., Full Professor, ENPC (CERMES, UR Navier), Université Paris Est, Marne-la-Vallee, France. e-mail: yujun.cui@enpc.fr.
Celso Romanel, Ph.D., Associate Professor, Departamento de Engenharia Civil, Pontifícia Universidade Católica do Rio de Janeiro, Rio de Janeiro, RJ, Brazil. e-mail: celso.romanel@gmail.com.
Submitted on February 1, 2012; Final Acceptance on May 12, 2015; Discussion open until December 31, 2015.

ing suction probes, such as tensiometer cavitation and psychrometer temperature effects.

In this paper changes of the in-situ soil state (moisture, suction and soil temperature) profiles due to climatic effects were predicted considering soil-atmosphere interactions in a water-limited environment. The principle of mass and energy conservation was applied to describe 1D water (liquid and vapour) and 1D heat flows in an unsaturated soil and a surface energy balance was imposed to the evaporation fluxes from a wet bare soil surface (Choudhury *et al.*, 1986; Xu & Qiu, 1997). A 1D explicit finite difference program (SAIAFDM model) developed at Ecole Nationale des Ponts et Chaussees (Gao, 2006) was used for numerical calculations.

The numerical calculations were carried out using the daily meteorological data collected by a French weather station, from 2004 to 2005. The soil parameters were determined from laboratory measurements by Fleureau *et al.* (2007) on soil specimens obtained at three different depths at studied region. Parametric analyses were carried out to estimate the influence of several parameters (soil albedo, saturated hydraulic conductivity, initial soil temperature profile, meteorological data) on the profile distributions, including fluctuations in the superficial zone of seasonal soil profile. Computed results were also compared with in situ soil temperature measurements in 2005 in Mormoiron, France.

2. Transient Water Flow in Unsaturated Soils

Consider a porous material, consisting of a solid matrix with a continuous pore space filled with fluid, a mixture of liquid water and vapour. For the particular case of one-dimensional water flow (along the vertical z direction), the flow of liquid water q_{wz} occurs in response to a hydraulic gradient that can be described by Darcy's law,

$$q_{wz} = -k_w(h_m)\frac{\partial(h_w)}{\partial z} \tag{1}$$

where the hydraulic conductivity k_w is a function of the matric suction head h_m. In the absence of an osmotic pressure head, the total hydraulic head h_w is defined as the sum of the matric head and the elevation head z,

$$h_w = h_m + z \tag{2}$$

The flow of water vapor q_{vz} in an unsaturated soil can be described by Fick's law (Fredlund & Dakshanamurthy, 1982) as:

$$q_{vz} = -\frac{1}{\rho_w} D_v \frac{\partial P_v}{\partial z} \tag{3}$$

where ρ_w is the water density at 20 °C (1000 kg/m^3), D_v the diffusion coefficient of the water vapour through the soil and P_v is the partial pressure due to water vapour.

Hence, the total flow of water q_z may be expressed as the sum of the liquid water flow q_{wz} and water vapour flow q_{vz} as:

$$q_z = -k_w \frac{\partial(h_w)}{\partial z} - \frac{1}{\rho_w} D_v \frac{\partial P_v}{\partial z} \tag{4}$$

Fredlund & Morgenstern (1976) suggested that the change in volumetric water content $\Delta V_w/V$ may be estimated through the following constitutive relationship:

$$\theta_w = \frac{\Delta V_w}{V} = [m_1^w d(\sigma_z - u_a) + m_2^w d(u_a - u_w)] \tag{5}$$

where σ_z is the vertical stress component, u_a the pressure in the air phase, u_w the pressure in the water phase, m_1^w the slope of the $d(\sigma_z - u_a)$ *vs.* volumetric water content plot for $d(u_a - u_w) = 0$ and m_2^w the slope of the $d(u_a - u_w)$ *vs.* volumetric water content plot for $d(\sigma_z - u_a) = 0$.

Assuming that there is no change in both vertical stress and air pressure,

$$d(\sigma_z - u_a) = 0 \tag{6a}$$

$$d(u_a - u_w) = -d(u_w) = -\rho_w g d(h_m) = -\rho_w g d(h_w - z) \tag{6b}$$

then the change in volumetric water content with respect to time may be written as:

$$\frac{\partial \theta_w}{\partial t} = -\rho_w g m_2^w \frac{\partial(h_w - z)}{\partial t} = -\rho_w g m_2^w \frac{\partial(h_w)}{\partial t} \tag{7}$$

However, the divergence of the total water flux in the one-dimensional space $\partial q_z / \partial z$ is equivalent to the change of volumetric water content with respect to time $\partial \theta_w / \partial t$. Hence from Eqs. 4 and 7 the following mass balance equation can be written,

$$\frac{\partial(\theta_w)}{\partial t} + \frac{\partial(q_z)}{\partial z} = 0 \tag{8}$$

$$\frac{\partial(h_w)}{\partial t} = C_w \frac{\partial}{\partial z}\left(k_w \frac{\partial h_w}{\partial z}\right) + C_v \frac{\partial}{\partial z}\left(D_v \frac{\partial P_v}{\partial z}\right) \tag{9}$$

where the modulus of volume change of the liquid water phase is given as:

$$C_w = \frac{1}{\rho_w g m_2^w} \tag{9a}$$

and the modulus of volume change of the vapour phase is defined as:

$$C_v = \frac{1}{(\rho_w)^2 g m_2^w}\left(\frac{P + P_v}{P}\right) \tag{9b}$$

The term $(P + P_v)/P$ is a correction factor introduced by Wilson (1990) to account for combined flow due to vapour diffusion and bulk air advection, where P is the total

atmospheric pressure and P_v the partial pressure in the soil due to water vapour. According to Wilson *et al.* (1994) this correction factor in most applications is approximately equal to unity and has little effect on the solution.

The two unknown variables of Eq. 9, namely the hydraulic head h_w and partial vapour pressure P_v, are not independent and may be related through a thermodynamic relationship (Edlefsen & Anderson, 1943),

$$P_v = P_{vs} h_T \tag{10}$$

where P_{vs} is the saturation vapour pressure at the soil temperature T and h_T is the relative humidity defined as:

$$h_T = \exp(h_m W_v / RT) \tag{11}$$

considering h_m the matric suction head, W_v the molecular mass of water (0.018 kg/mol), R the universal gas constant (8.314 J/(mol.K)) and T the absolute temperature (K).

Observe that calculation of the partial vapour pressure in Eq. 10 depends on the temperature, whose variation along the soil profile must be accounted for. Wilson (1990), Philip & De Vries (1957) and De Vries (1987) suggested the following equation for heat flow,

$$C_h \frac{\partial(T)}{\partial t} = \frac{\partial}{\partial z}\left(\lambda \frac{\partial T}{\partial z}\right) - L_v \frac{P + P_v}{P} \frac{\partial}{\partial z}\left(D_v \frac{\partial P_v}{\partial z}\right) \tag{12}$$

where C_h is the volumetric specific heat (J/(m^3 °C)), λ the apparent thermal conductivity of soil (W/(m^3 °C)) and L_v the latent heat of vaporization for water (J/kg) determined as:

$$L_v = 4.186 \times 10^3 (607 - 0.7T) \tag{13}$$

where T is given in °C.

The volumetric specific heat of the soil can be defined as follows (De Vries, 1963):

$$C_h = C_s \theta_s + C_w \theta_w + C_a \theta_a \tag{14}$$

where θ_w, θ_a and θ_s are the volumetric fractions of water, gas and solid materials, respectively, and C_w (4.15 x 10^6), C_a and C_s (2.24 x 10^6) their volumetric specific heat (J/m^3. °C). The value of C_a can be negligible (Gao, 2006).

The apparent thermal conductivity of soil λ can be also determined from De Vries (1963),

$$\lambda = \frac{f_s \theta_s \lambda_s + f_w \theta_w \lambda_w + f_a \theta_a \lambda_a}{f_s \theta_s + f_w \theta_w + f_a \theta_a} \tag{15}$$

where the thermal conductivity of water is $\lambda_w = 0.57$ W/m °C, the thermal conductivity of solids varies between $2.0 \le \lambda_s \le 7.7$ W/m °C depending on the quartz volumetric fraction (Johansen, 1975) and the thermal conductivity of the gaseous phase is composed by the conductivity of the dry air ($\lambda_{dryair} = 0.025$ W/m °C) plus the conductivity of the water vapour ($\lambda_{vapourr} = 0.608\theta_w$ W/m °C). The weighting coefficients $f_w = 1$ and f_a, f_s are estimated as (Gao, 2006):

$$f_s = \left[1 + \left(\frac{\lambda_s}{\lambda_w} - 1\right)\right]^{-1} \tag{16}$$

$$f_a = \frac{1}{3}\sum_{i=1}^{3}\left[1 + \left(\frac{\lambda_a}{\lambda_w} - 1\right) g_i\right]^{-1} \tag{17}$$

where the shape factors g_1, g_2 and g_3 may be estimated from the following correlations:

$$g_1 = g_2 = \frac{0.105 - 0.015}{0.121}\theta_w + 0.015 \tag{17a}$$

for $\theta_w \le 0.121$

$$g_1 = g_2 = \frac{0.333 - 0.105}{0.236 - 0.121}(\theta_w - 0.121) + 0.105 \tag{17b}$$

for $\theta_w > 0.121$

$$g_1 + g_2 + g_3 = 1 \tag{17c}$$

The governing equation for heat flow (Eq. 12) does not include the heat transfer by convection but several publications (Andersland & Anderson, 1978; Jame & Norum, 1980) point out that this contribution is negligible for most engineering applications.

Hence, the transfer of liquid, water vapour and heat in a porous medium is described by Eqs. 9, 10 and 12, respectively. The vapour pressure variable P_v is the common variable to all three equations.

3. Soil-Atmosphere Boundary Condition

The most direct method of estimating evapotranspiration is considering a surface energy balance. The net incoming solar radiation at any location is converted into heat energy, which warms the air above the surface and the soil itself, and into latent heat of evapotranspiration from the soil surface.

Consider R_n as the net radiation at the earth's surface, discounting the part of the incoming solar radiation R_{si} reflected by the surface albedo. Conservation of energy requires that the energy consumed by evaporation must equal that supplied, while conservation of mass requires that the rate at which water evaporates from the surface be equal to the rate at which it is dispersed into the atmosphere. According to Blight (2002, 2013) the surface energy balance, i.e. the way R_n is converted at the ground surface, may be expressed as:

$$R_n = L_e + H + G \tag{18}$$

where L_e is the latent energy transfer (positive for evaporation and negative for condensation), H is the sensible heat flux, the energy consumed in heating the air above the surface ("sensible" because this is the heat sensed or felt by the observer) and G is the soil heat flux (positive when energy is transferred to the near-surface soil and negative when energy is transferred to the atmosphere).

Equation 18 refers only to solar energy. If energy from an additional source is present (e.g. wind energy) a term describing this kind of energy should be included. For instance,

$$R_n + W_e = L_e + H + G \quad (19)$$

where W_e is the effective energy flux arising from the wind. In the case of landfills the heat supplied from the decomposing waste may also influence evaporation and should be added as a new term in the surface energy balance (Bendz & Bengtsson, 1996).

The net radiation flux R_n can be measured directly or estimated. Cui *et al.* (2010) calculated it from the incoming solar radiation R_{si} and the long-wave radiation emitted by soil surface and atmosphere, suggesting the following expression:

$$R_n = (1-a)R_{si} - \varepsilon_s \sigma T_s^4 + \varepsilon_a \sigma T_a^4 \quad (20)$$

where a is the soil albedo, ε_s the soil-surface emissivity, ε_a the air emissivity, σ the Stefan-Boltzmann constant (5.67 x 10^{-8} Wm^{-2} K^{-4}); T_s (K) and T_a (K) are the absolute soil surface and air temperatures, respectively. The soil albedo represents the ratio of reflected to incident solar radiation and it is a function of several surface parameters including soil color, water content, roughness and vegetation cover, usually being lower for wet and rough conditions. The albedo value ranges from 0 to 1. The value of 0 refers to a blackbody, a theoretical media that absorbs 100% of the incident radiation. Albedo ranging from 0.1 to 0.2 corresponds to dark-colored, rough soil surfaces, while the values around 0.4-0.5 indicate smooth, light-colored soil surfaces. The value of 1 refers to an ideal reflector surface in which all the energy falling on the surface is reflected. Solar altitude angle and soil moisture are the two main factors that influence the albedo value (Li & Hu, 2009).

In Eq. 18 the sensible heat flux H between soil and air is given by (Choudhury *et al.*, 1986; Kalma,1989):

$$H = \frac{\rho_a C_{pa}(T_s - T_a)}{r_a} \quad (21)$$

where ρ_a is air density, C_{pa} the specific heat of air at constant pressure equal to 1.013 x 10^3 J/(kg.K), T_s the absolute soil surface temperature (K) and T_a the absolute air temperature (K) at height z_a. The aerodynamic resistance r_a is the diffusion resistance to sensible heat transfer between the surface and height z_a; a reliable estimation of this parameter is important for soil-atmosphere interaction problems. Kalma (1989) observed good agreement between estimated and measured aerodynamic resistance over bare soil surface using Eq. 22 developed by Choudhury *et al.* (1986), based on an exact solution for stable conditions ($T_s < T_a$ and Richardson number $R_i > 0$) and on an approximate solution under unstable condition ($T_s > T_a$ and Richardson number $R_i < 0$) with a claimed 95% accuracy.

$$r_a = r_{a0} \frac{1}{(1 + R_i(T_s - T_a))^n} \quad (22)$$

where the exponent $\eta = 0.75$ is used for unstable conditions and $\eta = 2$ for stable conditions. The aerodynamic resistance r_{a0} is obtained from a logarithmic wind profile and may be calculated as:

$$r_{a0} = \frac{\left[\ln\left(\frac{z_a - d}{z_0}\right)\right]^2}{k^2 u_z} \quad (22a)$$

where u_z is the wind speed measured at height z_a, d the zero plane displacement equivalent to the vegetation height, z_0 the roughness length for momentum (wind) transfer and k the von Karman constant (0.41). When no vegetation is considered $d = 0$.

The Richardson number R_i in Eq. 22 is defined as:

$$R_i = \frac{g(T_a - T_s)(z_a - d)}{u_z^2 T_a} \quad (22b)$$

where g is the acceleration of gravity.

In Eq. 18 the latent heat flux L_e may be determined as (Xu & Qiu, 1997),

$$L_e = \frac{L_v M_w (P_{vz0} - P_{vza})}{RTr_a} \quad (23)$$

where L_v is the latent heat of vaporization, M_w the molecular mass of water equal to 0.018 kg/mol, P_{vz0} the partial vapour pressure at the soil surface, P_{vza} the partial vapour pressure in the air at height z_a, R the universal gas constant (8.314 J/(mol.K)) and T (K) the average absolute temperature $T = (T_a + T_s)/2$;

Finally, the soil heat flux G may be calculated from the energy balance equation (Eq. 18), considering the net radiation flux R_n (Eq. 20) and the energy fluxes calculated with Eqs. 21 and 23.

4. Constitutive Equations

Since in Eq. 1 the unsaturated hydraulic conductivity k_w depends on the matric suction head h_m, the following equation proposed by Juarez-Badillo (1975) was used in this research:

$$k_w = \frac{k_s}{1 + \left(\frac{k_s}{k_{w1}} - 1\right)\left(\frac{s}{s_1}\right)^{\xi}} \quad (24)$$

where k_s is the saturated hydraulic conductivity at suction $s = 0$, k_{w1} the unsaturated hydraulic conductivity at suction s_1 and ξ a parameter that controls the shape of the suction vs. unsaturated hydraulic conductivity curve s-k_w .

The equation for heat flow (Eq. 12) is a function of the volumetric specific heat C_h and the apparent thermal conductivity of soil λ which, by their turn, depend on the volu-

metric water content θ_w (Eqs. 14 and 15). Hence, it is necessary to establish a relationship between suction *s vs.* volumetric water content θ_w that, according to Juarez-Badillo (1975), may be written as:

$$\theta_w = \frac{\theta_{ws} - \theta_r}{1 + \left(\frac{\theta_{ws} - \theta_r}{\theta_{w1} - \theta_r} - 1 \right) \left(\frac{s}{s_1} \right)^{\varsigma}} + \theta_r \quad (25)$$

where θ_{ws} is the saturated volumetric water content, θ_r the residual volumetric water content, θ_{w1} the volumetric water content corresponding to suction s_1 and ς a parameter that controls the shape of the suction vs. volumetric water content curve s - θ_w called the soil-water characteristic curve or the soil water retention curve (SWRC). A number of equations have been suggested for the SWRC and almost all the equations suggested can be derived from a single generic form as presented by Leong & Rahardjo (1997). The equations represent the general sigmoidal shape of the SWRC as observed on the Eq. 25 used in this research.

5. Computer Program Based on a Finite Difference Method

In order to estimate the rate of evaporation at the ground surface, the computer program SAIAFDM was used to simultaneously solve the coupled equations of mass balance (liquid water and vapour), heat flow and energy balance between the soil and atmosphere. It was originally developed by Gao (2006) based on a 1D finite difference scheme and subsequently modified by Cui *et al.* (2005, 2010). The model assumes no variation in volume of voids as a function of the variation in suction or, in other words, the soil is considered as a rigid material.

The governing Eqs. 9 and 12 and can be rewritten as:

$$\frac{\partial (h_w)}{\partial t} = C_w \left(\frac{\partial k_w}{\partial z} \frac{\partial h_w}{\partial z} + k_w \frac{\partial^2 h_w}{\partial z^2} \right) + C_v \left(\frac{\partial D_v}{\partial z} \frac{\partial P_v}{\partial z} + D_v \frac{\partial^2 P_v}{\partial z^2} \right) \quad (9)$$

$$C_h \frac{\partial (T)}{\partial t} = \frac{\partial \lambda}{\partial z} \frac{\partial T}{\partial z} + \lambda \frac{\partial^2 T}{\partial z^2} - L_v \frac{P + P_v}{P} \left(\frac{\partial D_v}{\partial z} \frac{\partial P_v}{\partial z} + D_v \frac{\partial^2 P_v}{\partial z^2} \right) \quad (12)$$

Considering the forward difference scheme for first-order derivatives and a central difference scheme for second-order derivatives, the differential governing equations (Eqs. 9 and 12) can be approximated as:

$$\frac{h_w^{i,j+1} - h_w^{i,j}}{\Delta t} = C_w \left(\frac{k_w^{i+1,j} - k_w^{i,j}}{\Delta z} \times \frac{h_w^{i+1,j} - h_w^{i,j}}{\Delta z} + k_w \frac{h_w^{i+1,j} - 2h_w^{i,j} + h_w^{i-1,j}}{\Delta z^2} \right) + C_v \left(\frac{D_v^{i+1,j} - D_v^{i,j}}{\Delta z} \times \frac{P_v^{i+1,j} - P_v^{i,j}}{\Delta z} + D_v \frac{P_v^{i+1,j} - 2P_v^{i,j} + P_v^{i-1,j}}{\Delta z^2} \right) \quad (26)$$

$$C_h \frac{T^{i,j+1} - T^{i,j}}{\Delta t} = \frac{\lambda^{i+1,j} - \lambda^{i,j}}{\Delta z} \times \frac{T^{i+1,j} - T^{i,j}}{\Delta z} + \lambda \frac{T^{i+1,j} - 2T^{i,j} + T^{i-1,j}}{\Delta z^2} - L_v \frac{P + P_v}{P} \left(\frac{D_v^{i+1,j} - D_v^{i,j}}{\Delta z} \times \frac{P_v^{i+1,j} - P_v^{i,j}}{\Delta z} + D_v \frac{P_v^{i+1,j} - 2P_v^{i,j} + P_v^{i-1,j}}{\Delta z^2} \right) \quad (27)$$

where the index i is associated to the vertical coordinate z and the index j to time.

The advantage of using the approximate Eqs. 26 and 27 is that $h_w^{i,j+1}$ and $T^{i,j+1}$ can be calculated explicitly but, as its main disadvantage, the numerical solution may become unstable when time and space increments are not well chosen. In this research the time increment was selected as $\Delta t = 5$ s and the space increment was delimited by $5 \text{ mm} \leq \Delta z \leq 50 \text{ mm}$ for stable and accurate results. Figure 1 gives a general view of the program framework.

6. Data Presentation

6.1. Site description and input data

The investigated site is located in Mormoiron, department of Vaucluse, in the southeast of France. It has a Mediterranean climate. The site was instrumented by the French research office on geology and mines (BRGM) and the measured soil temperature is used to evaluate the numerical simulations. Cui *et al.* (2010) mention that previous geotechnical investigations to a depth of 10 m showed that the soil layer is relatively uniform, composed of clay of green colour.

The daily meteorological data were available from a French weather station, called Carpentras station, that is located at about 10 km from Mormoiron site. The data include precipitation, relative humidity of the air, air temperature, solar radiation and wind speed measured at 2 m from the soil surface from January 1964 to December 2000 (a total of 42 years). The Mormoiron site was selected for studying because a water deficit is observed in most of time throughout the monitored years where the recharge of the

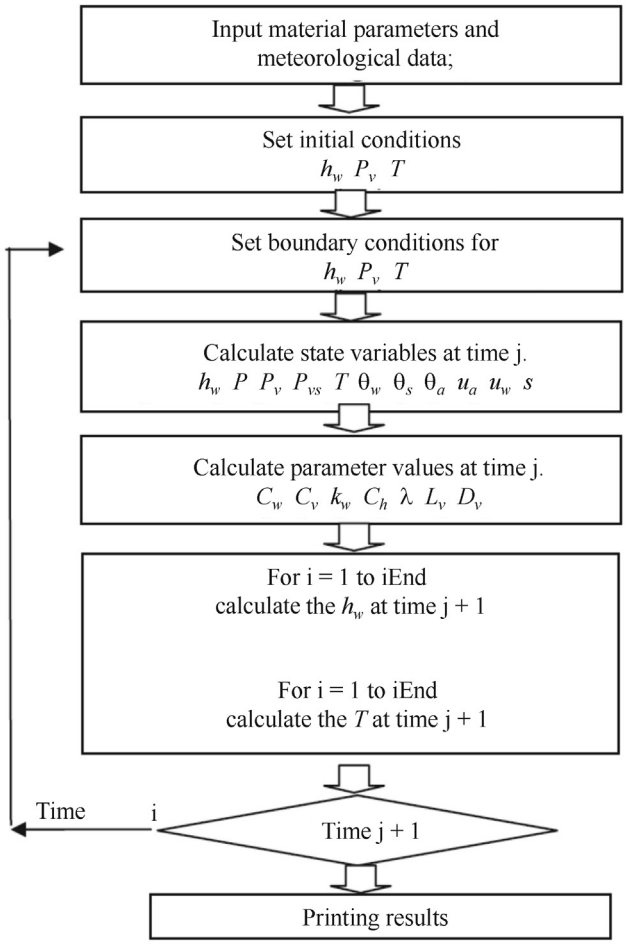

Figure 1 - The program framework used in the present study.

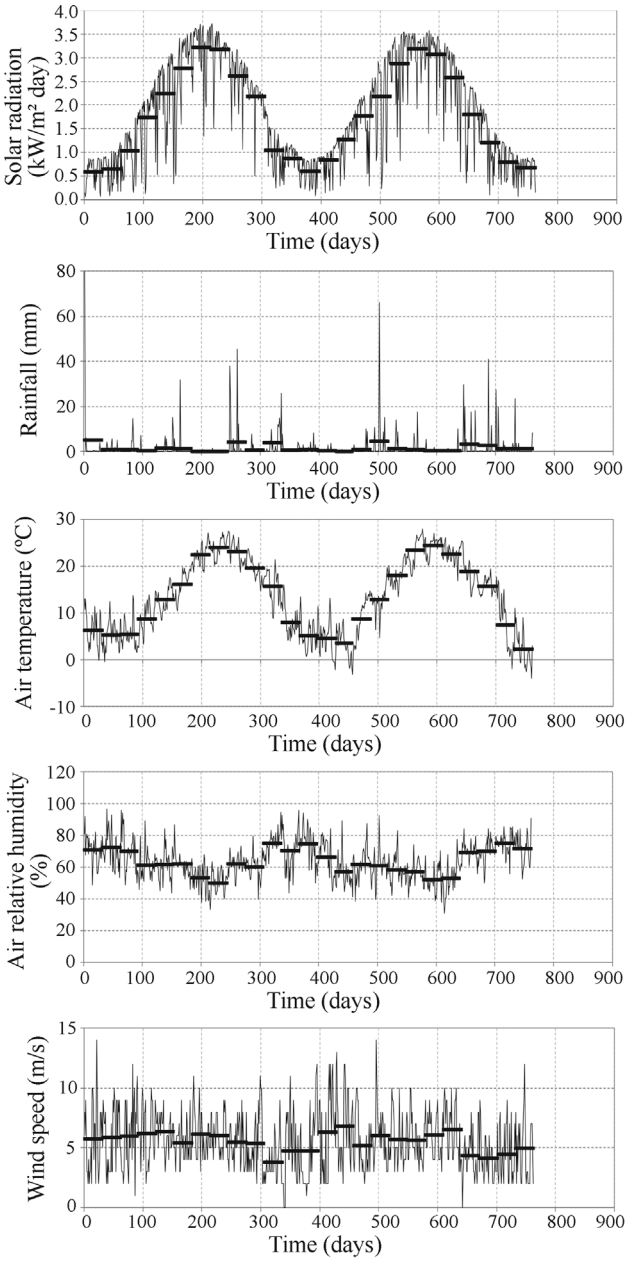

Figure 2 - Variation of the daily measured solar radiation, rainfall, air temperature, air relative humidity and wind speed for the 2 year time period.

water table did not take place and the zone of unsaturated soil assumed a much greater significance. Examination of the recorded meteorological data showed that a seasonal warming trend is observed in the recorded data after the year 2000 (mean maximum and minimum annually air temperatures equal to 21.2 °C and 8.3 °C respectively).

The climatic data at the Mormoiron site in France was recorded daily from December 1, 2003 to December 31, 2005, consisting of solar radiation (0.05 to 0.35 kWm^2), rainfall (0 to 60 mm), air temperature (0 to 25 °C), air relative humidity (40 to 90%) and wind speed (2 to 14 m/s), as shown by plots in Fig. 2 where the average monthly values were also indicated by the horizontal bars. It should be observed that the air temperature changes correlate well with solar radiation while the air relative humidity does not necessary follow the rainfall pattern. The air relative humidity depends not only on precipitation, but also on air temperature and wind speed (Cui & Zornberg, 2008). A water deficit is observed in most of time throughout the two years, except for brief periods in December 2003, October 2004, April 2005 and October 2005. Thus, the years of 2004 and 2005 correspond to drier conditions where the recharge of the water table did not take place and the zone of unsaturated soil assumed a much greater significance.

The actual land soil cover was represented by a two-layer system of homogeneous soils with an upper layer thickness Z_1 = 3.45 m, maximum depth Z_{max} = 5.25 m (Fig. 3) and soil albedo 0.15. For both layers the parameters related to the flow of liquid and water vapour are listed in Tables 1 to 4. The initial temperature profile and the initial volumetric water content profile, corresponding to the beginning of the analysis on December 1, 2013 (late Fall), are shown in Figs. 4 and 5, which have been estimated from field measurement taken at the Mormoiron site.

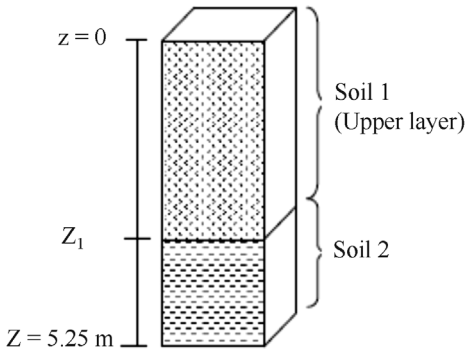

Figure 3 - The two-layer system of homogeneous soils.

7. Parametric Analyses

In the following sensitivity analyses, only one parameter is changed independently at each time while the remaining parameters are kept constant ignoring the effects of parameters interactions and output or responses interdependences. This simple approach facilitates a preliminary identification of potentially important parameters for further researches that will take into account the interdependence between model parameters or the interactions between model outputs or responses. Moreover the interdependence of the investigated parameters is not observed for the considered magnitude variations.

7.1. Influence of the initial temperature profile

In order to investigate the effects of the initial temperature profile on the volumetric water content and soil temperature distribution, a 5 °C increase was prescribed to all points along the profile of Fig. 4, based on an expected daytime temperature oscillation. However, as can be observed in Fig. 6 the volumetric water content profile remained insensitive to the initial temperature variation (T and T + 5 °C). Values for the volumetric water content (and suction) were practically constant for depths z > 1.5 m. The dependence of the soil temperature on the soil water retention curve was not considered.

Figures 7 and 8 present the predicted soil temperature profiles from January to July 2004 considering the two hypotheses for the initial temperature profile. It can be observed that close to the surface (0-10 cm) the soil temperatures are slightly affected (1 °C to 2 °C only) by the initial profiles, adjusting to the air temperature quickly. At deeper depths (z > 1.5 m) the temperatures tend to become stable over the year and preserving the original difference of 5 °C imposed on the initial temperature profiles. For instance, at z = 3 m the soil temperature approaches the initial

Table 1 - Soil-water retention function input variables.

Parameter	$Z \le Z_1$	$Z_1 < Z \le Z_{max}$	Unity
Saturated volumetric water content θ_{ws}	0.490	0.400	m^3/m^3
Suction s_1	700	200	kPa
Residual volumetric water content θ_r	0.080	0.080	m^3/m^3
Volumetric water content θ_{w1} at suction s_1	0.240	0.240	m^3/m^3
Shape parameter ς	1.1	1.1	-

Table 2 - Unsaturated hydraulic conductivity function input variables.

Parameter	$Z \le Z_1$	$Z_1 < Z \le Z_{max}$	Unity
Saturated hydraulic conductivity k_s	$1.2x10^{-11}$	$2.4x10^{-10}$	m/s
Suction s_1	40	40	kPa
Unsaturated hydraulic conductivity k_{w1} at suction s_1	$1.2x10^{-14}$	$1.2x10^{-14}$	m/s
Shape parameter ξ	1.25	1.25	-

Table 3 - Volumetric specific heat input variables.

Parameter	$Z \le Z_1$	$Z_1 < Z \le Z_{max}$	Unity
Solid specific heat C_s	$2.24x10^6$	$2.24x10^6$	J/m^3 °C
Water specific heat C_w	$4.15x10^6$	$4.15x10^6$	J/m^3 °C
Air specific heat C_a	0	0	J/m^3 °C

Table 4 - Thermal conductivity input variables.

Parameter	$Z \leq Z_1$	$Z_1 < Z \leq Z_{max}$	unity
Thermal conductivity λ_s of solids	3.92	3.92	W/m °C
Thermal conductivity λ_w of water	0.57	0.57	W/m °C
Thermal conductivity λ_a of air	$0.025+0.608\theta_w$	$0.025+0.608\theta_w$	W/m °C

temperatures 12 °C < T < 13 °C and 16 °C < T + 5 < 17 °C. These results suggest that for the soil near the surface it is not relevant to know the values of initial temperature with high accuracy, but for deeper layers this is an important question.

7.2. Influence of the saturated hydraulic conductivity

The saturated hydraulic conductivities of the two-layer system were modified in order to verify their effects on the volumetric water content and suction profiles. The values listed in Table 2 were increased a hundredfold passing from $k_S^A = 1.2\times10^{-11}$ m/s for $Z \leq 3.5$ m and $k_S^A = 2.4\times10^{-10}$ m/s for $Z > 3.5$ m (herein identified as case A) to $k_S^B = 1.2\times10^{-9}$ m/s for $Z \leq 3.5$ m and $k_S^B = 2.4\times10^{-8}$ m/s for $Z > 3.5$ m (denominated as case B). McCartney & Parks (2009) reported that empirical predictions can lead to an error in hydraulic conductivity of 1 to 4

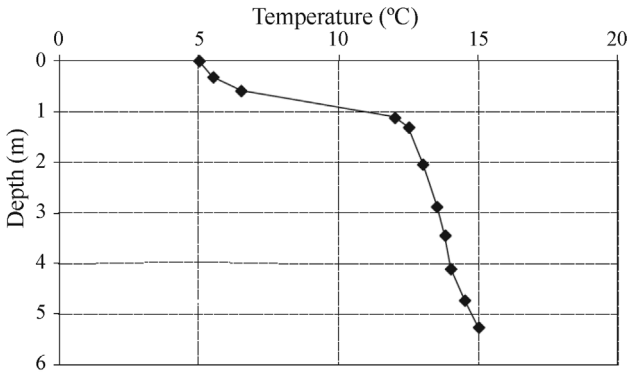

Figure 4 - Initial temperature profile on December 1, 2003.

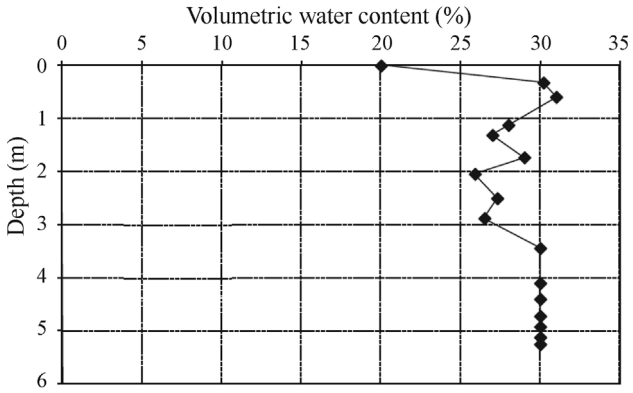

Figure 5 - Initial volumetric water content profile on December 1, 2003.

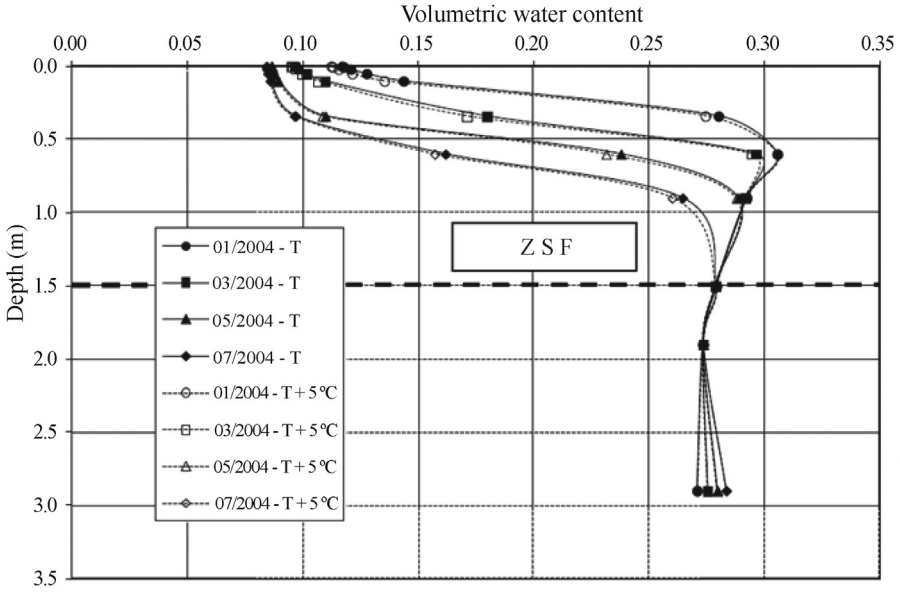

Figure 6 - Volumetric water content profile from January to July/2004 considering the initial temperature profiles T (solid line) and T + 5 °C (dotted line).

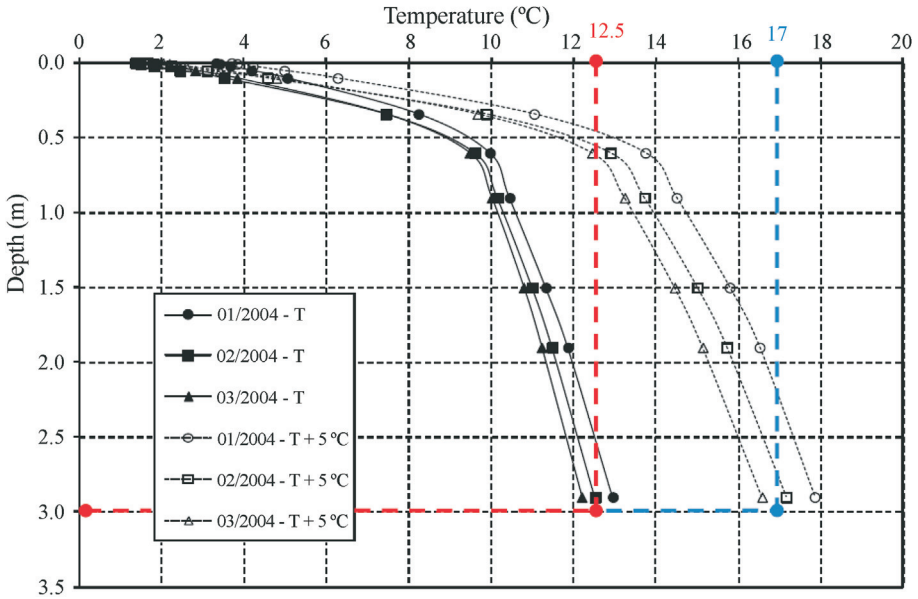

Figure 7 - Soil temperature profile from January to March/2004 considering the initial temperature profiles *T* (solid line) and *T* + 5 °C (dotted line).

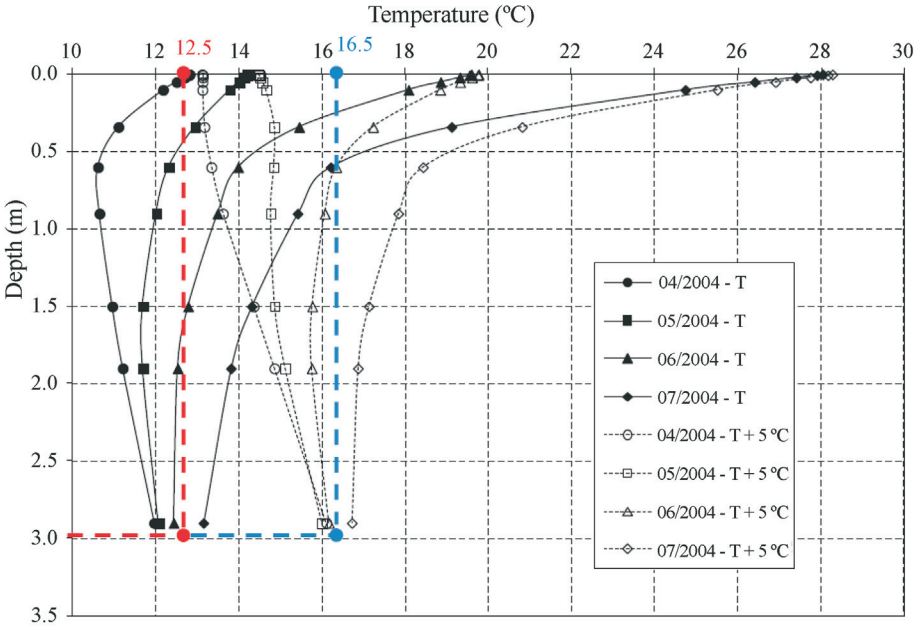

Figure 8 - Soil temperature profile from April to July/2004 considering the initial temperature profiles *T* (solid line) and *T* + 5 °C (dotted line).

orders of magnitude, with the greatest discrepancies at low moisture contents.

The results are presented in Fig. 9 in terms of suction profiles. Their insensitivity to changes of the saturated hydraulic conductivities is quite apparent since curves from both cases are coincident. The same behavior was observed when comparing the volumetric water content and soil temperature profiles. Although the computed evaporative fluxes are very sensitive to the permeability of the soil (Wilson, 1990), the years of 2004 and 2005 correspond to drier conditions (high suction values), and it seems that changes of this magnitude on the saturated hydraulic conductivities have not significant effect on the suction-unsaturated hydraulic conductivity relationship.

7.3. Influence of the upper layer thickness

This parametric analysis investigated the influence of the upper layer thickness (Fig. 3), considering in case A a

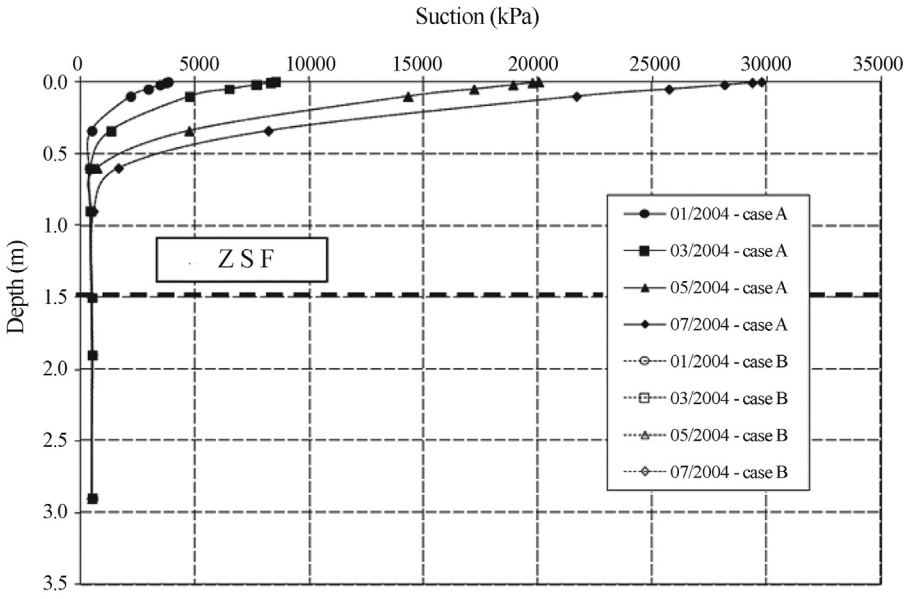

Figure 9 - Influence of the saturated hydraulic conductivity on suction profiles from January to July/2004.

thickness $Z_1 = 3.45$ m and in case C a new value $Z_1 = 0.5$ m. With respect to previous analyses, this means that the soil between depths 0.5 m < z < 3.45 m had its hydraulic properties changed (soil-water retention function and unsaturated hydraulic conductivity function) according to the values listed in Tables 1 and 2. The soil was divided into two layers with variable thickness to account for the observed changes of the hydraulic properties in the laboratory measurements.

Predicted results for both cases can be seen in Fig. 10. It can be concluded that the differences observed between distributions are small except in the superficial region between 0.40 m < z < 0.90 m (marked in blue) that was more affected by the climatic conditions. The results also indicated that the expected hysteresis in the functions due to the variation of the wetting and drying processes in the field has not significant effect on the predicted soil profiles in Mormoiron, France.

7.4. Influence of the soil albedo

The changes in soil profiles during a given period depend on the ratio of reflected to incident solar radiation (i.e., the soil albedo value). The sensitivity of predicted temperature changes to variations of soil albedo is studied next,

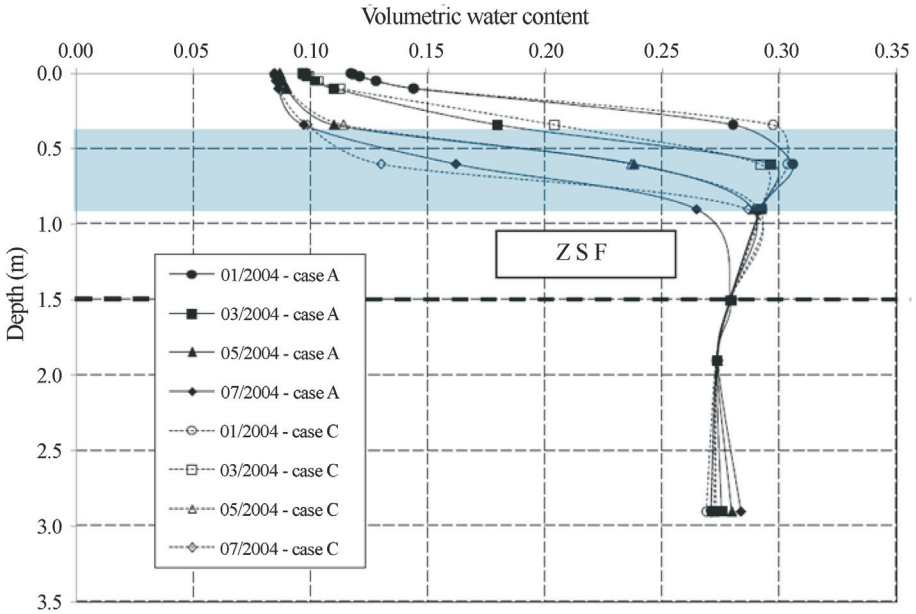

Figure 10 - Influence of upper layer thickness on volumetric water content profiles from January to July/2004.

considering soil albedo values of 0.15 (case A) and 0.05 (case D).

Figures 11 shows that the soil temperatures profiles are not significantly affected by the soil albedo values, mainly during the cold season (from January to March, 2005). During the warmer months (from April to August 2005) it may observed for case D small temperature increases (approximately 1 °C) probably due to the higher incident solar radiation that made the soil albedo parameter more relevant for analysis of temperature distributions.

7.5. Influence of the climatic data frequency

Figures 6, 9 and 10 show that the soil layer where moisture and corresponding suction profiles influenced by climatic conditions is about 1.5 m deep but Figs. 7 and 8 indicate that the layer where the soil temperature profile is affected by climate is thicker (3 m). Therefore the zone in which the interchange of water between the atmosphere and the soil occurs is different from the one in which the interchange of heat between the atmosphere and the soil takes place.

Whereas the impact of thermal variation on the soil behavior is recognized and especially significant for fined grained soils and higher temperature values (Lingnau *et al.*, 1996, Tang & Cui, 2005), Franchomme *et al.* (2013) demonstrated that temperatures variations from 1 °C to 30 °C do not significantly affect the measured soil shear stress parameters for a kaolinite-sand mixture.

For the particular site of Mormoiron, France, the zone of seasonal fluctuations (ZSF) in which water contents change seasonally due to climate changes can be established as 1.5m deep considering the variations through the cold and warm seasons (January to July 2004). For London clay with vegetation the ZSF is about 1.0 m according to Smethurst *et al.* (2006).

In order to investigate the influence of the climatic data frequency (input data), some analyses were repeated considering data sampled at a monthly frequency (case E) instead of the daily frequency adopted in Case A. The monthly frequency refers to the average values shown in Fig. 2 as horizontal bars.

Predicted results for suction profiles are shown in Fig. 12. It can be observed that for the monthly frequency case the ZSF doubled in size, reaching the depth of 3 m, and the suctions profiles for cases A and E are quite discrepant. Similar results were predicted for soil temperature and volumetric water content profiles.

These unexpected results have probably come from the simple and rather naïve choice of converting a daily time series into a monthly time series just by averaging the recorded values within a 30-days period. Specific conversion functions must be applied for an adequate collapse of a daily data sequence to a monthly time series, but it is quite common in the practice of engineering to represent a monthly interval by its average value. When dealing with time series, this issue may be quite important especially when the recorded climatic data (rainfall, wind speed, air temperature, air relative humidity) are not all sampled at the same frequency.

7.6. Comparison between predicted and measured soil temperatures

Figure 13 presents the comparison between predicted and measured changes in soil temperature at three different depths (0.5 m, 1.5 m, and 2.5 m) from January to August 2005 in Mormoiron, France. The results suggest that near the soil surface the predictions were less satisfactory, due probably to vegetation or other effects, such as soil cracking, not considered in the computational model. A sensitivity analysis of soil temperature and water content profiles to

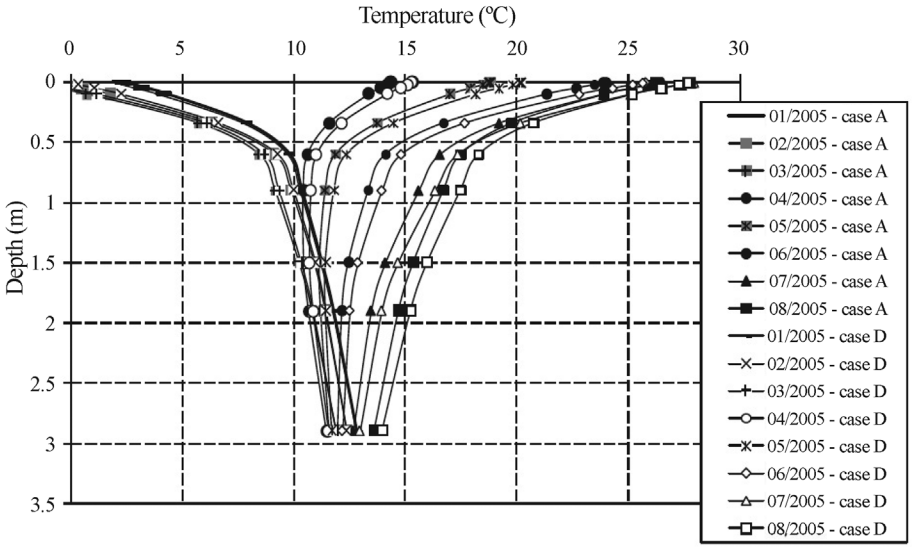

Figure 11 - Influence of soil albedo values on soil temperature profiles from January to August/2005.

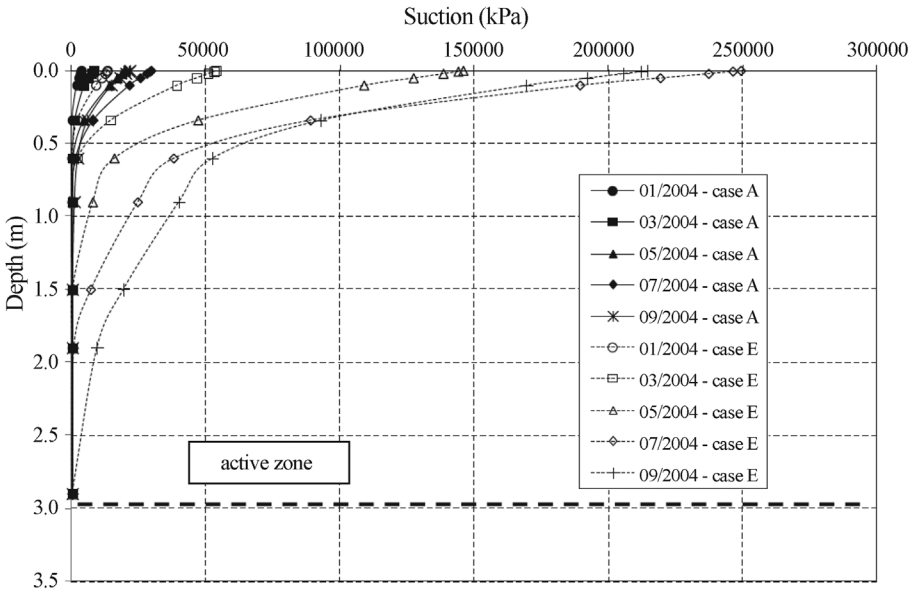

Figure 12 - Influence of climatic data frequency on suction profiles from January to September/2004.

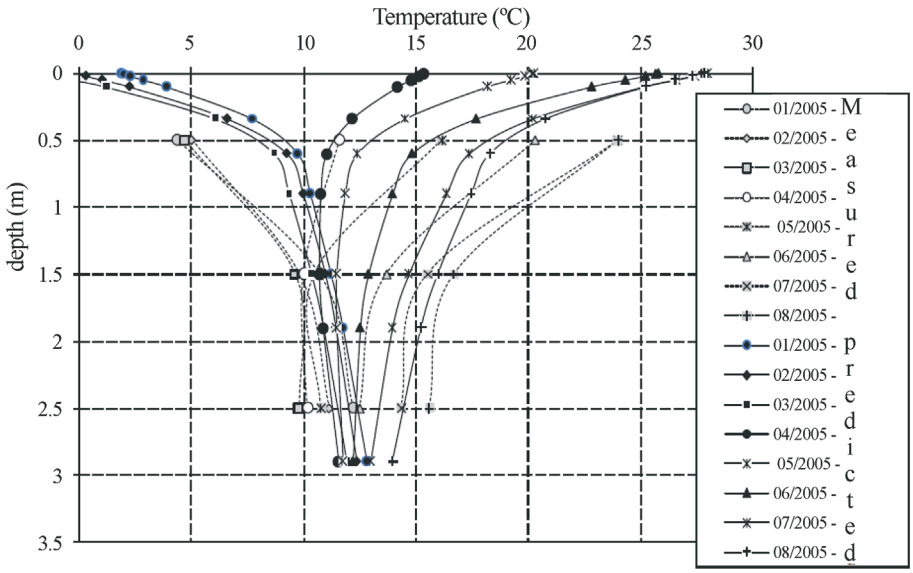

Figure 13 - Comparison between predicted and measured soil temperatures from January to August/2005.

variations of other unknown parameters (such as soil water content that depend on the soil temperature) should also be investigated. Cui *et al.* (2005) suggested considering the superficial zone as an independent layer with its own and particular values of soil parameters.

8. Conclusion

This paper investigated the influence of soil-atmosphere interactions on an unsaturated soil in water-limited environment using a coupled heat-water flow model with a balance of net solar energy at earth's surface. The numerical calculations were carried out using the daily meteorological data collected by a French weather station, from 2004 to 2005. The soil parameters were determined from laboratory measurements on soil specimens obtained at three different depths at the studied region.

Numerical results were obtained by approximating the governing partial differential equations through a 1-D finite difference scheme representing the soil as a two-layer system. Parametric analyses estimated the effects on soil state profiles caused by changes in initial conditions, hydraulic properties, model geometry, ratio of reflected to incident solar radiation and characteristics of meteorological data.

The results suggest that for the soil near the surface it is not relevant to know the values of initial temperature with high accuracy, but for deeper layers this is an important question. For the investigated site, the zone of seasonal fluctuations (ZSF) where the moisture and corresponding suction profiles are influenced by climatic conditions is about 1.5 m although the layer where the soil temperature is affected by climatic conditions is twice this value (3 m). The results also show that calculated average month meteorological values as daily inputs significantly modify the ZSF (about 100%) but the response depends on the statistical procedure to convert a daily time series into a representative monthly sequence.

The comparison of predicted and measured changes in soil state temperature profiles suggest that in near the surface layers the simulations are less satisfactory probably due to vegetation effects or other mechanical phenomena such as soil cracking. Further investigations, including experimental studies and numerical simulations, are needed to better understand climate effects on soil state profiles and their influence on geotechnical engineering problems.

Acknowledgments

The first authors are grateful for sponsorship by the Brazilian government agencies CNPq and CAPES. This work has been performed within the French ANR-RGCU project: ARGIC. The meteorological data was provided by Météo France and the soil data by BRGM. The helpful comments and corrections by the reviewers are also appreciated.

References

Andersland, O. & Anderson, D. (1978). Geotechnical Engineering for Cold Regions. McGraw-Hill. Inc., New York.

Bendz, D. & Bengtsson, L. (1996). Evaporation from an active, uncovered landfill: Journal Hydrology, 182:1, p. 143-155.

Blight, G.E. (1997). Interactions between the atmosphere and the earth. Géotechnique, 47:4, p. 715-767.

Blight, G.E. (2002). Measuring evaporation from soil surfaces for environmental and geotechnical purposes. Water SA, 28:4, p. 381-394.

Blight, G. E. (2013). Unsaturated Soil Mechanics in Geotechnical Practice. CRC Press, Taylor & Francis Group, London, 597 p.

Choudhury, B.J.; Reginato, R.J. & Idso, S.B. (1986). An analysis of infrared temperature observations over wheat and calculation of latent heat flux. Agric. For. Meteorol., 37:2, p. 75-88.

Cui, Y.J.; Lu, Y.F.; Delage, P. & Riffard, M. (2005). Field simulation of in site water content and temperature changes due to ground-atmospheric interactions. Géotechnique, 55:7, p. 557-567.

Cui, Y.J. & Zornberg, J. (2008). Water balance and evapotranspiration monitoring in geotechnical and geoenvironmental engineering. Geotechnical and Geological Engineering, 26:6, p. 783-798.

Cui, Y.J.; Gao, Y. B. & Ferber, V. (2010). Simulating the water content and temperature changes in an experimental embankment using meteorological data. Engineering Geology, 141:3, p. 456-471.

Dai, A.; Lamb, P.J.; Trenberth, K.R.; Hulme, M.; Jones, P. D. & Xie, P. (2004). The recent Sahel drought is real. Int. J. Climatol., 24:11, p.1323-1331.

De Vries, D.A. (1963). Thermal properties of soils. In: W.R. Van Wijk (ed) Physics of Plant Environment. North-Holland, Amsterdam, pp 210-235.

De Vries, D.A. (1987). The theory of heat and moisture transfer in porous media revisited. International Journal of Heat and Mass Transfer, 30:7, p.1343-1350.

Edlefsen, N.E. & Anderson, A.B.C. (1943). Thermodynamics of soil moisture. Hilgardia 15:2, p. 31-298.

Federer, C.A.; Vörösmarty, C. & Fekete, B. (1996). Inter comparison of methods for calculating potential evaporation in regional and global water balance models. Water Resources Research, 32:1, p. 2315-2321.

Fetter, C.W. (1994). Applied Hydrogeology. 3rd ed. Macmillan College Publishing, Inc., New York, 616 p.

Fleureau, J.M.; Guellati, Z.; Nguyen, D. & Souli H. (2007). Synthèse des essais réalisés au LMSSMat sur le matériau du site de Mormoiron, Annexe de rapport BRGM, Projet ANR-05-PRGCU-005, Rapport d'activité n° 3, École Centrale de Paris.

Franchomme, G.; Rosin-Paumier, S. & Masrouri, F. (2013). Evaluating the impact of thermal variations on the penetration test parameters, Proc. The 1st Pan American Conference on Unsaturated Soils, Cartagena de Indias, Colombia , pp. 371-376.

Fredlund, D.G. & Morgenstern, N.R. (1976). Constitutive relations for volume change in unsaturated soils, Canadian Geotechnical Journal, 13:3, p.261-276.

Fredlund, D. G. & Dakshanamurthy, V. (1982). Transient flow process in unsaturated soils under flux boundary conditions. Proc. the 4th International Conference on Numerical Methods in Geomechanics, Edmonton, Canada, pp. 307-317.

Gao, Y.B. (2006). From Meterological Data to the Predication of Embankment Stability. Technical report, CERMES-ENPC, Paris, 180 p.

Gens, A. (2010). Soil-environment interactions in geotechnical engineering. Géotechnique, 60:1, p. 3-74.

Jame, Y.W. & Norum, D.I. (1980). Heat and mass transfer in a freezing unsaturated porous medium. Water Resources Research, 16:4, p. 811-819.

Johansen, O. (1975). Thermal Conductivity of Soils. Ph.D. Thesis, Trondheim, Norway, CRREL Draft Translation 637, ADA 044002.

Juárez-Badillo E. (1975). Constitutive relationships for soils, Proc. Symposium on Recent Developments in the Analysis of Soil Behavior and their Application to Geotechnical Structures, University of New South Wales, Australia, pp. 231-257.

Kalma, J.G. (1989). A Comparison of Expressions for the Aerodynamic Resistance to Sensible Heat Transfer. CSIRO Division of Water Resources, Technical Memorandum, 89/6, 18 p.

Leong, E.C. & Rahardjo, H. (1997). Permeability functions for unsaturated soils. J. Geotech. Geoenviron. Eng., 123:12, p. 1118-1126.

Li, Y. & Hu, Z. (2009). A study on parameterization of surface albedo over grassland surface in the northern Tibetan Plateau, Adv. Atmos. Sci., 26:1, p. 161-168.

Lingnau, B.E.; Graham, J.; Yarechewski, D.; Tanaka, N. & Gray, M.N. (1996). Effects of temperature on strength and compressibility of sand-bentonite buffer, Engineering Geology, 41:1, p. 103-115.

McCartney, J. S. & Parks, J. (2009). Uncertainty in predicted hydraulic conductivity functions of unsaturated soils. Proc. 17th International Conference on Soil Mechanics and Geotechnical Engineering, Alexandria, Egypt. Taylor & Francis Group, London, pp. 1618-1621.

Penman, H.L. (1948). Natural evaporation from open water, bare soil and grass. Proceedings of the Royal Society of London, Series A, 193:1032, p. 120-145.

Philip, J.R. 7 de Vries, D.A. (1957). Moisture movement in porous materials under temperature gradients. Transactions American Geophysical Union, 38:2, p. 222-232.

Priestley, C.H.B. & Taylor, R.J. (1972). On the assessment of surface heat flux and evaporation using large-scale parameters. Monthly Weather Review, 100:2, p. 81-92.

Skidmore, E.L.; Jacobs, H.S. & Powers, W.L. (1969). Potential evapotranspiration as influenced by wind. Agron. J., 61:4, p. 543-546.

Smethurst, J.; Clarke, D. & Powrie, W. (2006). Seasonal changes in pore water pressure in a grass covered cut slope in London Clay. Géotechnique, 56:8, p. 523-537.

Tang, A.M. & Cui, Y.-J. (2005). Controlling suction by the vapour equilibrium technique at different temperatures and its application in determining the water retention properties of MX80 clay, Canadian Geotechnical Journal, 42:1, p. 287-296.

Wilson, G.W. (1990). Evaporation from Bare Soil Surfaces. Ph.D. Thesis, University of Saskatchewan, Saskatoon, Canada.

Wilson, G.W.; Fredlund, D.G. & Barbour S.L. (1994). Coupled soil-atmosphere modeling for soil evaporation. Canadian Geotechnical Journal, 31:2, p.151-161.

Xu, Q. & Qiu, C.-J. (1997). A variational method for computing surface heat fluxes from ARM surface energy and radiation balance system. J. of App. Meteorology, 36:1, p. 3-11.